

Doubly-adaptive autoregressive Kalman filter for GNSS carrier tracking under scintillation conditions

Sergi Locubiche-Serra, Gonzalo Seco-Granados, José A. López-Salcedo
Department of Telecommunications and Systems Engineering
Universitat Autònoma de Barcelona (UAB), Spain
Email: sergi.locubiche@uab.cat, gonzalo.seco@uab.cat, jose.salcedo@uab.cat

Abstract—In Global Navigation Satellite Systems, receivers have to cope with ionospheric scintillation, which is of paramount importance for high-precision positioning applications. However, the design of robust carrier tracking techniques under these conditions still remains an open problem. The time-varying correlated scintillation phase can be modeled as an AR(p) process, whose linear nature fits very well into the linear Kalman filter formulation and can be embedded into its architecture. State-of-the-art techniques stand for fixed architectures optimized for very specific scenarios, namely the KF-AR(1). In this paper, a new adaptive KF-AR(p) approach with new implementations with high order AR models (AR-2, AR-3) is proposed so as to match better the input scintillation time series in time-varying scenarios, which also include the presence of AWGN noise. Simulation results are provided to show the enhanced performance and adaptability in these scenarios compared to previous approaches such as the standard Kalman filter and the KF-AR(1).

I. INTRODUCTION

Carrier tracking is one of the nuclear tasks to be carried out in a GNSS receiver, and the exploitation of carrier phase measurements is of paramount importance for high-precision positioning applications, since they do provide ultraprecise positioning information. So far, most of the existing GNSS receivers are implementing carrier tracking using the well-known phase-locked loop (PLL) technique [1]. However, despite its maturity and widespread deployment, conventional PLL techniques are facing new challenges due to the increasing need of extending the use of GNSS receivers beyond the limits of their original open-sky designs. On the one hand, this is a result of the commercial push for providing ubiquitous positioning capabilities to user mobile terminals. This involves moving GNSS receivers to the urban and soft-indoor arena, where propagation impairments and time-varying working conditions abound. On the other hand, the expansion of GNSS in emerging countries has unveiled the need to cope with ionospheric scintillation, which is a frequent impairment in equatorial regions [2] and poses serious concerns to the widespread deployment of GNSS in those areas.

Conventional PLL-based carrier tracking is known to experience serious troubles in the presence of the above-mentioned challenges. However, PLL techniques are known to be nothing

but a particularization of the Kalman filter [3], which is well-known to outperform the previous techniques. The Kalman filter makes use of the general framework of optimal minimum mean square error (MMSE) estimation, and therefore becomes the best way to optimally perform carrier tracking in GNSS receivers. The use of Kalman filters in GNSS carrier tracking can be seen as the natural improvement to cope with the challenges to be faced by next-generation GNSS receivers.

The presence of scintillation disturbances often introduces deep fades together with abrupt phase changes, the so-called canonical fades. Thus, the design of robust adaptive carrier tracking techniques to deal with it becomes of paramount importance. Scintillation time series can be modeled through a linear model such as the class of autoregressive (AR) random processes. The approaches so far account for a Kalman filter with an AR augmentation in its formulation to deal with both dynamics and scintillation phase in a decoupled manner [4]. However, its fixed architecture is optimized for very specific scenarios, but makes it not suitable for others, due to the time-varying nature of scintillation events, or when scintillation is absent. On the other hand, a simple AR(1) model may not be sufficient to model all kinds of scintillation. As an example, it is found that, for severe scintillation, AR(1), AR(2) and AR(3) models are found to fit pretty well the power spectral density (PSD) of the actual input scintillation phase. In contrast, for moderate scintillation the PSD departs from an AR(1) model, which suggests that AR(2) or eventually AR(3) models provide a better fit to moderate scintillation phase. Even the presence of additive white Gaussian noise (AWGN) may cause the scintillation time series to be better fitted by higher order AR models.

Under these premises, in this contribution, 1) the Kalman filter formulation is extended to incorporate a generic AR(p) model to cope with scintillation disturbances in the presence of AWGN noise, 2) an adaptive KF-AR(p) approach is presented to estimate the AR parameters that provide the best matching with the current input scintillation time series, 3) a doubly-adaptive KF-AR approach is presented, consisting in: 3.1) a switching mechanism to estimate the AR model order best matching the input working conditions, 3.2) a method to counteract the deep fades that appear in the presence of severe scintillation, based on the actual C/N_0 .

This work was partly supported by the Spanish Government under grant TEC2014-53656-R and by the European Space Agency (ESA) under the ROCAT contract AO/1-6918/11/NL/AT.

II. STATEMENT OF PROBLEM AND SIGNAL MODEL

The ionospheric electron density irregularities are known to affect GNSS signals by introducing rapidly time-varying amplitude fades and phase variations. This poses a serious concern to the operation of GNSS receivers, since they are prone to suffer from severe carrier phase jitter and to fall into frequent losses of lock.

Autoregressive (AR) random processes are a useful class of random time series that are obtained by filtering white Gaussian noise through an all-pass filter. Let the scintillation phase at time n be denoted by ψ_n . The time-domain representation of an AR scintillation phase model is given by (1),

$$\psi_n = \sum_{k=1}^p \beta_k \psi_{n-k} + s_n \quad (1)$$

where p is the order of the AR process, referred to as AR(p), $\{\beta_k\}_{k=1}^p$ are the filter coefficients and $s_n \sim \mathcal{N}(0, \sigma_s^2)$ is the zero-mean white Gaussian driving noise with variance σ_s^2 [5].

III. KALMAN FILTER AUTOREGRESSIVE (KF-AR)

At the phase level, a correlated Gaussian distribution is often considered as a first-order approximation to model scintillation disturbances [6]. This observation is of interest for the application of Kalman filter-based carrier tracking techniques, which can therefore take advantage of the optimality properties of the Kalman filter in the presence of Gaussian disturbances, and thus encompass scintillation disturbances in a natural manner. The approach adopted herein is to focus on the estimation of the scintillation phase disturbance in such a way that once estimated, it can be removed from the input carrier phase by decoupling both the carrier phase dynamics and scintillation phase.

The objective of this section is to extend the standard Kalman filter formulation to the case of carrier phase tracking in the presence of scintillation disturbances. This can easily be done by taking advantage of the linear nature of AR random processes stated before, which fits very well into the linear Kalman filter formulation.

A. AR(p) state-space system model

According to the signal model introduced in Section II, an AR(p) random process can be represented using the recursion shown before in (1). In matrix form, this expression leads to the state-space model in (2),

$$\psi_{n,p} = \begin{bmatrix} \beta_1 & \beta_2 & \beta_3 & \cdots & \beta_p \\ 1 & 0 & 0 & \cdots & 0 \\ 0 & 1 & 0 & \cdots & 0 \\ \vdots & 0 & \vdots & \ddots & \vdots \\ 0 & \cdots & 0 & 1 & 0 \end{bmatrix} \psi_{n-1,p} + \begin{bmatrix} 1 \\ 0 \\ 0 \\ \vdots \\ 0 \end{bmatrix} s_n \quad (2)$$

with $\psi_{n,p} \doteq [\psi_n \ \psi_{n-1} \ \psi_{n-2} \ \cdots \ \psi_{n-p+1}]^T$ the $(p \times 1)$ state-space vector of the AR(p) random process, and $s_n \sim \mathcal{N}(0, \sigma_s^2)$ the model noise. From this state-space representation, a constant $(p \times p)$ transition matrix $\mathbf{F}_{\psi,p}$ and a constant $(p \times 1)$ model noise matrix $\mathbf{G}_{\psi,p}$ can be identified, respectively

in (3) and (4). These matrices allow the state-space model for an AR(p) random process in (2) to be represented as (5).

$$\mathbf{F}_{\psi,p} \doteq \begin{bmatrix} \beta_1 & \beta_2 & \beta_3 & \cdots & \beta_p \\ 1 & 0 & 0 & \cdots & 0 \\ 0 & 1 & 0 & \cdots & 0 \\ \vdots & 0 & \vdots & \ddots & \vdots \\ 0 & \cdots & 0 & 1 & 0 \end{bmatrix} \quad (3)$$

$$\mathbf{G}_{\psi,p} \doteq [1 \ 0 \ 0 \ \cdots \ 0]^T \quad (4)$$

$$\psi_{n,p} = \mathbf{F}_{\psi,p} \psi_{n-1,p} + \mathbf{G}_{\psi,p} s_n \quad (5)$$

B. Carrier dynamics and AR(p) state-space system model

For the problem at hand, it is considered that the carrier phase is evolving according to the carrier dynamics (*i.e.* user dynamics) and the phase scintillation disturbance that can be modeled as an AR(p) random process. Regarding the former, the time-varying evolution of the carrier phase θ_n can be approximated through a third-order Taylor series expansion,

$$\theta_n \approx \theta_{n-1} + T\dot{\theta}_{n-1} + \frac{1}{2!}T^2\ddot{\theta}_{n-1} + \frac{1}{3!}T^3\ddot{\theta}_{n-1} \quad (6)$$

where T is the sampling time, and $\dot{\theta}(n)$, $\ddot{\theta}(n)$, $\ddot{\theta}(n)$ are the carrier frequency, frequency rate and frequency jerk (*i.e.* the first, second and third derivatives of the carrier phase). For a third order model, (6) can be represented in matrix form as the state-space model in (7), in normalized notation,

$$\mathbf{x}_n = \begin{bmatrix} 1 & 1 & 1/2 \\ 0 & 1 & 1 \\ 0 & 0 & 1 \end{bmatrix} \mathbf{x}_{n-1} + \begin{bmatrix} 1/6 \\ 1/2 \\ 1 \end{bmatrix} v_{n-1} \quad (7)$$

with $\mathbf{x}_n \doteq [\theta_n \ T\dot{\theta}_n \ T^2\ddot{\theta}_n]^T$ the (3×1) state-space vector of the carrier phase dynamics, and $v_n \doteq T^3\ddot{\theta}_n$ the model noise accounting for the missing higher order terms. Similarly to Section III-A, a constant (3×3) transition matrix \mathbf{F}_θ and a constant (3×1) model noise matrix \mathbf{G}_θ are identified, allowing the state-space model for the carrier phase dynamics to be represented as (8).

$$\theta_n = \mathbf{F}_\theta \theta_{n-1} + \mathbf{G}_\theta v_n \quad (8)$$

At this point, the state-space system model for user dynamics in (8) can be merged with the one for AR(p) scintillation disturbance in (5) into the augmented system in (9), which can be expressed in compact form as (10). Expression (10) becomes the core of the so-called Kalman filter autoregressive (KF-AR).

$$\begin{bmatrix} \theta_n \\ \psi_{n,p} \end{bmatrix} = \begin{bmatrix} \mathbf{F}_\theta & \mathbf{0}_{3 \times p} \\ \mathbf{0}_{p \times 3} & \mathbf{F}_{\psi,p} \end{bmatrix} \begin{bmatrix} \theta_{n-1} \\ \psi_{n-1,p} \end{bmatrix} + \begin{bmatrix} \mathbf{G}_\theta & \mathbf{0}_{3 \times 1} \\ \mathbf{0}_{p \times 1} & \mathbf{G}_{\psi,p} \end{bmatrix} \begin{bmatrix} v_n \\ s_n \end{bmatrix} \quad (9)$$

$$\mathbf{x}_{n,p} = \mathbf{F}_p \mathbf{x}_{n-1,p} + \mathbf{G}_p \mathbf{u}_{n,p} \quad (10)$$

The state transition is degraded by the presence of the model noise $\mathbf{u}_{n,p}$, which propagates to the rest of the Kalman states through \mathbf{G}_p . This noise affecting the transition equation is modeled as a zero-mean Gaussian process with covariance matrix,

$$\mathbf{Q}_{n,p} \doteq \begin{bmatrix} \sigma_v^2 \mathbf{G}_\theta \mathbf{G}_\theta^T & \mathbf{0}_{3 \times p} \\ \mathbf{0}_{p \times 3} & \sigma_s^2 \mathbf{G}_{\psi,p} \mathbf{G}_{\psi,p}^T \end{bmatrix} \quad (11)$$

On the other hand, taking into account that the Kalman filter deals with scalar phase measurements, the Kalman measurement model is (12),

$$z_n = \theta_n + \psi_n + w_n = [\mathbf{H}_\theta \quad \mathbf{H}_{\psi,p}] \mathbf{x}_{n,p} + w_n \quad (12)$$

with $\mathbf{H}_\theta = [1 \ 0 \ 0]$ and $\mathbf{H}_{\psi,p} = [1 \ 0_{p-1}^T]$ the user dynamics and scintillation observation matrices, and $w_n \sim \mathcal{N}(0, R_n)$ the measurement noise whose variance R_n corresponds to the phase noise at the discriminator output.

IV. ADAPTIVE HARD-LIMITED KALMAN FILTER WITH ADAPTIVE AUTOREGRESSIVE MODEL (AHL-KF-A2R)

The name AHL-KF-A2R is given by the different new implementations proposed here, which are detailed next. The block diagram of the AHL-KF-A2R is shown in Figure 1.

A. Estimation of scintillation parameters

The problem of fitting a given random process to an AR(p) model boils down to the problem of determining the set of filter coefficients $\{\beta_k\}_{k=1}^p$. Such problem can be addressed following two approaches, namely the Yule-Walker equations or the least squares or linear prediction method. Both are equivalent AR estimation methods [7]. However, the Yule-Walker method is presented herein because of its simplicity.

The recursion in (1) can be expressed in terms of the autocorrelation of the AR process given by $r_\psi(k) \doteq E[\psi_{n+k}\psi_n^*]$ resulting in the so-called Yule-Waker equations. In matrix form, these equations can conveniently be expressed as (13), which can be denoted as (14),

$$\begin{bmatrix} r_\psi(0) & r_\psi(1) & \cdots & r_\psi(p-1) \\ r_\psi(1) & r_\psi(0) & \cdots & r_\psi(p-2) \\ \vdots & \vdots & \ddots & \vdots \\ r_\psi(p-1) & r_\psi(p-2) & \cdots & r_\psi(0) \end{bmatrix} \begin{bmatrix} \beta_1 \\ \beta_2 \\ \vdots \\ \beta_p \end{bmatrix} = \begin{bmatrix} r_\psi(1) \\ r_\psi(2) \\ \vdots \\ r_\psi(p) \end{bmatrix} \quad (13)$$

$$\mathbf{R}_\psi \boldsymbol{\beta} = \mathbf{r}_\psi \quad (14)$$

where the autocorrelation of the random process under analysis, $r_\psi(k)$, can be estimated from the available measurements at the carrier phase discriminator output as (15),

$$\hat{r}_\psi(k) = \frac{1}{N} \sum_{n=0}^{N-1} \psi_{n+k} \psi_n^* \quad (15)$$

Substituting (15) into (13), the system can be solved for the unknown coefficients as (16). Once the filter coefficients are known, the driving noise variance can be obtained as (17),

$$\hat{\boldsymbol{\beta}} = \hat{\mathbf{R}}_\psi^{-1} \hat{\mathbf{r}}_\psi \quad (16)$$

$$\hat{\sigma}_s^2 = \hat{r}_\psi(0) - \sum_{k=1}^p \hat{\beta}_k \hat{r}_\psi(k) \quad (17)$$

The purpose of the following analysis is two-fold. On one hand, it is important to estimate the scintillation parameters, so that the Kalman filter is adaptively configured to match the actual input working conditions. The Kalman filter will be processing the input samples and applying some corrections to the local signal replica at the same time, thus having some

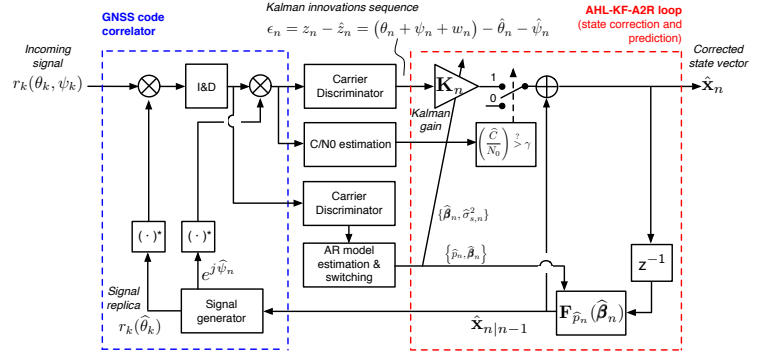


Fig. 1: Block diagram of the adaptive hard-limited Kalman filter with adaptive autoregressive model (AHL-KF-A2R).

effect on the next samples to be processed. Thus, the “online” performance of the AR model estimation discussed above is compared to an “offline” (*i.e.* theoretical) realization in the sense that the input samples are directly processed, with no Kalman filtering involved at all. On the other hand, the presence of AWGN is an important problem because it causes the resulting (*i.e.* aggregated) random process to be better fitted by high order AR(p) processes such as AR(2) or AR(3), or even to depart from an AR model.

This is the case of Figure 2 for severe scintillation using an AR(2) model. As the C/N_0 increases, $\beta_1 \rightarrow -1$ and $\beta_2 \rightarrow 0$, thus tending to an AR(1) process in the absence of AWGN (*i.e.* C/N_0 of 55 dB-Hz and beyond). However, in the presence of AWGN (*i.e.* C/N_0 below 50 dB-Hz), the values of β_1 and β_2 depart from the previous consideration, which proves the need for higher order AR models under these circumstances.

As for the estimation performance, it can be concluded from Figure 2 that the online KF-AR(2) estimator is performing correctly, since the estimated scintillation coefficients match the theoretical values. Figure 3 drives to the same conclusion. It shows the comparison between the offline and online estimation of σ_s^2 , for both moderate and severe scintillation. The only remark is that for severe scintillation, there is a small mismatch between both estimations for C/N_0 of 40 dB-Hz and beyond. This is expected to some extent, since severe scintillation poses difficulties for the Kalman filter to estimate σ_s^2 precisely, due to the abrupt variations of the input samples.

B. Switching AR model

Higher AR models can easily be obtained according to (14), and in some circumstances they may provide a tighter approximation to scintillation time series. Hence, it is of interest to extend the AR modeling of scintillation time series to higher model orders such as AR(2) and AR(3), already considered in Section IV-A. In these circumstances, having three possible models to work with, namely AR(1), AR(2), AR(3), it is clear that a selection mechanism is needed in order to choose the best model to be used at every time, and to switch from one model to the other. This gives raise to the KF-A2R technique. Determining the correct order of a statistical model is a well-known problem in the field of signal processing and

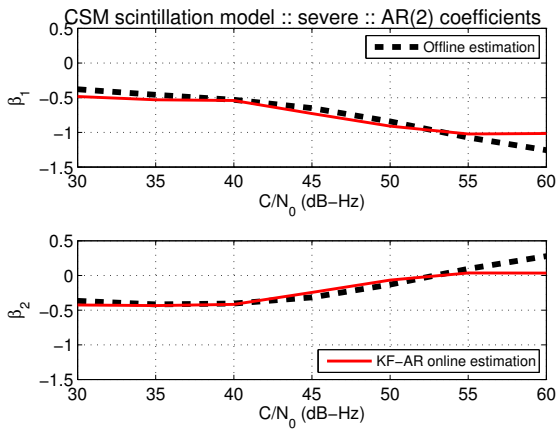


Fig. 2: Estimation of the AR(2) scintillation coefficients for severe scintillation time series.

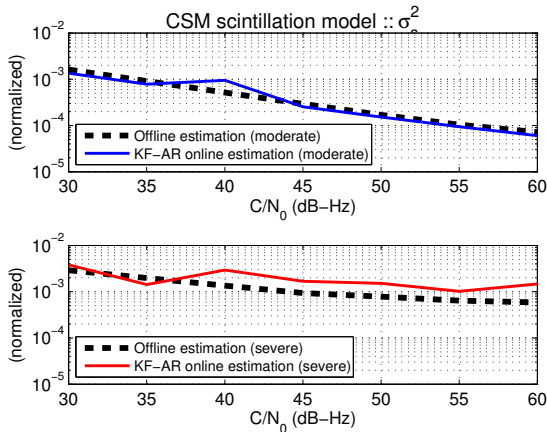


Fig. 3: Estimation of the AR(2) driving noise power for moderate (upper plot) and severe (lower plot) scintillation time series.

often referred to as model-order selection [8]. From (1), the signal model for the problem at hand can be formulated as (18),

$$\psi = \Psi_p \beta_p + s_p \quad (18)$$

where ψ is the $(N \times 1)$ vector of input samples to be fitted to some AR model, Ψ_p is the $(N \times p)$ matrix containing time-shifted replicas of the input samples, β_p is the vector of $(p \times 1)$ AR coefficients corresponding to some AR(p) model, and s_p is a zero-mean noisy $(N \times 1)$ vector with unknown noise power $\sigma_{s_p}^2$ that can be understood as the model mismatch errors for this particular problem. Assuming these errors to be Gaussian distributed, the likelihood function for the problem at hand becomes (19),

$$f_p(\psi | \beta_p, \sigma_{s_p}^2) = \frac{1}{(2\pi)^{\frac{N}{2}} \sigma_{s_p}^N} e^{-\frac{1}{2\sigma_{s_p}^2} \|\psi - \Psi_p \beta_p\|^2} \quad (19)$$

which depends on the unknown set of AR(p) coefficients β_p and the model mismatch error power $\sigma_{s_p}^2$. The maximum

likelihood estimates of both unknowns become (20) and (21),

$$\hat{\beta}_p = \left(\Psi_p^T \Psi_p \right)^{-1} \Psi_p^T \psi \quad (20)$$

$$\hat{\sigma}_{s_p}^2 = \frac{1}{N} \left\| \psi - \Psi_p \hat{\beta}_p \right\|^2 \quad (21)$$

Using these estimates, the compressed log-likelihood function becomes (22),

$$-2 \log f_p(\psi | \hat{\beta}_p, \hat{\sigma}_{s_p}^2) = C + N \log \hat{\sigma}_{s_p}^2 \quad (22)$$

for some irrelevant constant C . Once the compressed log-likelihood function is available, different model order selection criteria can be applied to determine the most likely model order \hat{p} , such as the Akaike, MAP, or MDL (also referred to as BIC–Bayesian information criterion) [8]. In the sequel, the minimum description length (MDL) is adopted, since it is found to be a consistent criterion [9]. The MDL criterion finds the most likely model order \hat{p} as (23),

$$\hat{p}_{\text{MDL}} = \arg \min_p J_{\text{MDL}}(p) \quad (23)$$

where after some mathematical process, the MDL cost function is given by (24), with $\hat{\sigma}_{s_p}^2$ obtained from (17).

$$J_{\text{MDL}}(p) = N \log \hat{\sigma}_{s_p}^2 + p \log N \quad (24)$$

C. Estimation of C/N_0

The measurement noise covariance matrix R_n is one of the parameters playing a key role in the Kalman filter performance. An interesting point is that the Kalman formulation explicitly indicates the time dependence of this matrix through the subindex n , thus allowing this matrix to be dynamically adjusted to match the actual working conditions. On the other hand, the presence of canonical fades caused by scintillation is a major source of loss-of-lock. In these circumstances, the performance of the Kalman filter will be severely degraded. From the Kalman filter perspective, these type of measurements have a rather nonlinear nature, and thus it is difficult to deal with them with a linear approach.

An alternative, though, would be to estimate the instantaneous C/N_0 of the received signal, and to use this information to update R_n accordingly in the computation of the Kalman gains. For the problem at hand, R_n is indeed a scalar term, and for the four-quadrant arctangent discriminator, R_n can be obtained from the received C/N_0 as (25),

$$\hat{R}_n = \frac{1}{2T \left(\frac{\hat{C}}{N_0} \right)_n} \left(1 + \frac{1}{2T \left(\frac{\hat{C}}{N_0} \right)_n} \right) \quad (25)$$

with $\left(\frac{\hat{C}}{N_0} \right)_n$ the estimated C/N_0 and T the predetection integration time at the code correlator.

Based on the estimated C/N_0 , the adaptive hard-limited (AHL) KF relies on the use of \hat{R}_n to update the Kalman equations, but implements instead a hard-limiting of the value of \hat{R}_n such that,

$$\begin{cases} R_n = \hat{R}_n, & \text{if } \left(\frac{\hat{C}}{N_0} \right)_n \geq \gamma \\ R_n = \Gamma, & \text{otherwise} \end{cases} \quad (26)$$

for some threshold γ that is empirically set at $\gamma = 25$ dB-Hz for the application under analysis, and with $\Gamma \rightarrow \infty$, thus causing $K_n = 0$. In this case, the corrected state vector \hat{x}_n is computed using the internal state-space model, only, and thus it gets isolated from the carrier discriminator output. In this way the Kalman filter is protected from abnormal measurements, and the loss-of-lock performance can be improved. For this purpose, the C/N_0 needs to be estimated and the narrow-wideband power ratio estimator (NWPR) is used herein.

The NWPR estimator can be found in detail in [10], and it is briefly summarized here. It is based on the fact that the noise power at the prompt correlator output can be analysed on two different noise bandwidths, see (27) and (28),

$$\text{WBP}_n = \sum_{m=1}^M |y_{n-m}|^2 \quad (27)$$

$$\text{NBP}_n = \left| \sum_{m=1}^M y_{n-m} \right|^2 \quad (28)$$

where WBP is the $1/T$ wideband noise power and NBP is the $1/MT$ narrowband noise power, M is the length of a sliding window within which the C/N_0 is estimated at a given time instant n , and y_n is the prompt correlator output. Based on these estimated powers, the mean of the power ratio can be computed using an exponential filter that weights through some constant α the estimates in previous time instants and the new estimates, as (29), and the C/N_0 can be finally estimated through expression (30),

$$\hat{\mu}_n = \alpha \left(\frac{\text{NBP}_n}{\text{WBP}_n} \right) + (1 - \alpha) \hat{\mu}_{n-1} \quad (29)$$

$$\left(\frac{\hat{C}}{N_0} \right)_n = \frac{1}{T} \frac{\hat{\mu}_n - 1}{M - \hat{\mu}_n} \quad (30)$$

When estimating the C/N_0 through the NWPR method, two trade-offs are dealt with. On one hand, the constant α is a trade-off between the estimator convergence time and the accuracy of the estimates in steady state regime. The parameter is set to $\alpha = 0.95$ herein. On the other hand, the value of M has the trade-off that: if M is too large, the averaging may be too large to detect spurious deep fadings, and thus R_n will not be adapted properly; if M is too small, the estimated C/N_0 may change too rapidly so as to make the Kalman filter unstable. As a rule of thumb, M is selected herein to be 0.25 seconds.

V. SIMULATION RESULTS

In this section, simulations are carried out to compare the original KF techniques with the improved ones proposed in this document. Two scenarios are selected as representative of real cases for static user, with small relative motion between the user and the satellites caused by the movement of the latter. In particular, a Doppler shift of 10 Hz, Doppler rate of 1 Hz/s and Doppler jerk of $2 \cdot 10^{-4}$ Hz/s² are considered. The scintillation time series are generated using the Cornell

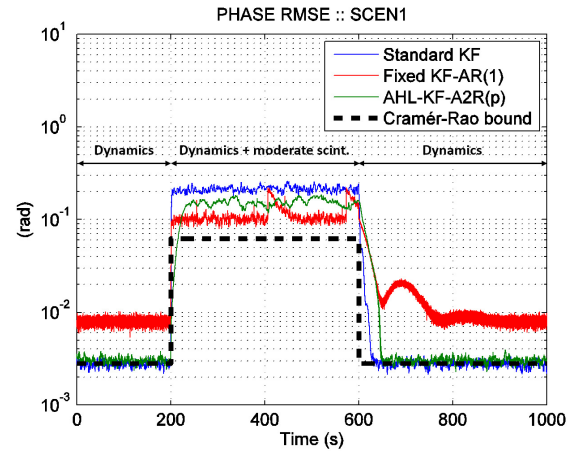


Fig. 4: Phase RMSE for standard KF, KF-AR(1) and AHL-KF-A2R(p) with model order switching mechanism for SCEN1.

Scintillation Model (CSM), with moderate ($S_4 = 0.5$, $\tau_0 = 0.8$) and severe ($S_4 = 0.8$, $\tau_0 = 0.4$) scintillation. For these, to configure the KF-AR(1), the AR(1) driving noise variance σ_s^2 can be in the range of $3 \cdot 10^{-4}$ and $1 \cdot 10^{-3}$ in normalized units, whereas β_1 can be in the range of $(-1, -0.95]$. Simulations are carried out for 100 Monte Carlo iterations.

A. SCEN1

This scenario simulates a real case where scintillation suddenly appears at a given moment, and after a while it disappears. The time-varying conditions refer to no-moderate-no scintillation following the pattern specified in Figure 4, which also shows the phase RMSE for the standard Kalman filter, the KF-AR(1) and the AHL-KF-A2R(p).

The standard Kalman filter is the technique showing the best performance when scintillation is absent, whereas in the presence of scintillation, it shows the worst performance, since the carrier phase state absorbs both the dynamics and scintillation phase. In the absence of scintillation, the AHL-KF-A2R technique is able to mostly select an AR(0) model (*i.e.* standard KF with no AR augmentation), and consequently it attains the performance lower bound. The technique also deals pretty well with moderate scintillation. However, in this region with moderate scintillation, the AHL-KF-A2R is outperformed by the fixed KF-AR(1). This may be due to the fact that the AR(1) parameters already implemented within this technique match pretty well the moderate scintillation events considered. In contrast, estimation of the AR(p) parameters in the AHL-KF-A2R inevitably contain errors, which introduce some additional jitter in the RMSE. But despite of this fact, the KF-AR(1) shows the worst performance in the absence of scintillation, caused by the fact that introducing an unnecessary AR model into the Kalman filter configuration also introduces some additional jitter. Moreover, when stepping from moderate to no scintillation, it takes a huge time to stabilize the phase RMSE. According to Figure 6 top, in the presence of moderate scintillation, the switching mechanism selects mainly either

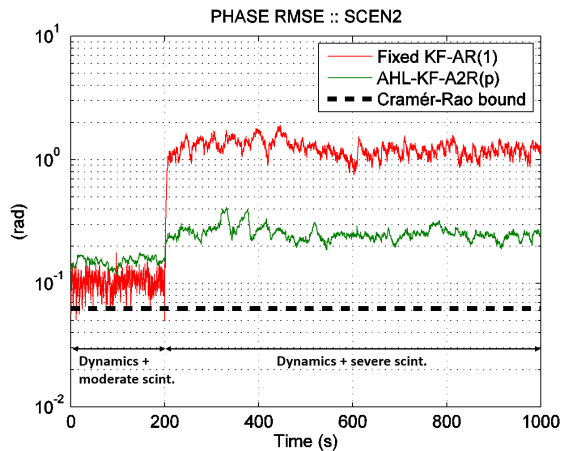


Fig. 5: Phase RMSE for KF-AR(1) and AHL-KF-A2R(p) with model order switching mechanism for SCEN2.

KF-AR configuration	Loss-of-lock probability
KF-AR(1)	0.79
AHL-KF-A2R(p)	< 0.01

TABLE I: Probability of loss-of-lock for KF-AR(1) and AHL-KF-A2R(p).

AR(2) or AR(3) models, and barely selects AR(1). This is also in agreement with the theoretical statements, where moderate scintillation is not properly modelled by an AR(1) process.

B. SCEN2

This scenario simulates a real case where moderate scintillation is present, and at a given time it gets stronger. The time-varying conditions refer to moderate-severe scintillation following the pattern specified in Figure 5, which also shows the phase RMSE for the KF-AR(1) and AHL-KF-A2R techniques. Table I shows their probabilities of loss-of-lock.

In the presence of severe scintillation, the AHL-KF-A2R clearly outperforms the KF-AR(1) technique. The KF-AR(1) shows a huge phase RMSE, which is considerably reduced by the AHL-KF-A2R, and a probability of loss-of-lock above 70%, whereas the AHL-KF-A2R is able to deliver a probability of loss-of-lock below 1%. Thus, it is proven that the AHL-KF-A2R introduces significant improvements over the KF-AR(1) in both metrics, and it delivers a much better performance. According to Figure 6 bottom, in the presence of severe scintillation, all AR model orders are selected, which is in agreement with the theoretical statement that severe scintillation can be fairly modelled by different model orders. Depending on the particular input working conditions (*i.e.* local effects of scintillation time series, presence of AWGN), some models may be more adequate than others at given time instants, and this is what is reflected in Figure 6 bottom.

VI. CONCLUSION

A new Kalman filter-based approach has been presented for next-generation GNSS receivers to deal with time-varying

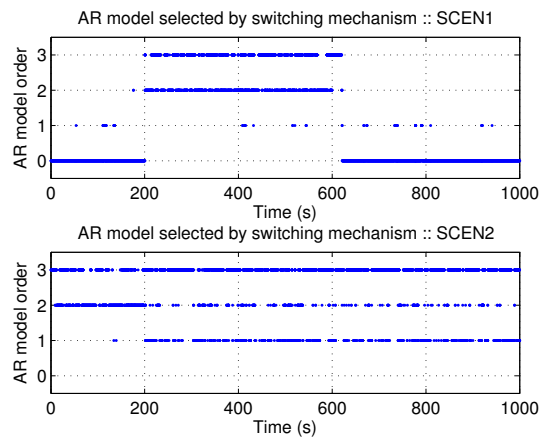


Fig. 6: Selection of AR(p) models as a function of time for AHL-KF-A2R.

ionospheric scintillation. Firstly, the Yule-Walker equations are used to estimate the scintillation parameters, so that the Kalman filter is adapted to fit the actual input working conditions. An AR model order switching mechanism by analysing the MDL cost function has been presented to select the most appropriate AR model at each time instant. Lastly, a C/N_0 estimator has been also included to adapt the Kalman filter in the presence of canonical fades caused particularly by severe scintillation. Simulations have been carried out in two representative time-varying scenarios, and simulation results have shown the goodness and enhanced performance of the proposed implementations.

REFERENCES

- [1] S. C. Gupta, "Phase-locked loops," *Proceedings of the IEEE*, vol. 63, no. 2, pp. 291–306, Feb 1975.
- [2] P. M. Kintner, T. E. Humphreys, and J. Hinks, "GNSS and ionospheric scintillation. How to survive the next solar maximum," *Inside GNSS*, pp. 22–33.
- [3] D. Polk and S. Gupta, "Quasi-Optimum Digital Phase-Locked Loops," *IEEE Transactions on Communications*, vol. 21, no. 1, pp. 75–82, Jan 1973.
- [4] J. Vilà-Valls, J. A. López-Salcedo, and G. Seco-Granados, "An interactive multiple model approach for robust GNSS carrier phase tracking under scintillation conditions," in *Acoustics, Speech and Signal Processing (ICASSP), 2013 IEEE International Conference on*, May 2013, pp. 6392–6396.
- [5] S. Kay, *Fundamentals of statistical signal processing. Vol I: Estimation theory*. Prentice Hall, 1993.
- [6] T. E. Humphreys, M. L. Psiaki, B. M. Ledvina, A. P. Cerruti, and P. M. Kintner, "Data-Driven Testbed for Evaluating GPS Carrier Tracking Loops in Ionospheric Scintillation," *IEEE Transactions on Aerospace and Electronic Systems*, vol. 46, no. 4, pp. 1609–1623, Oct 2010.
- [7] P. Stoica and R. Moses, *Spectral analysis of signals*. Prentice Hall, 2005.
- [8] P. Stoica and Y. Selen, "Model-order selection: a review of information criterion rules," *IEEE Signal Processing Magazine*, vol. 21, no. 4, pp. 36–47, July 2004.
- [9] P. M. Djuric and S. M. Kay, "Spectrum estimation and modeling," in *The digital signal processing handbook, 2nd edition*, V. K. Madisetti, Ed. CRC Press, 2010, ch. 14.
- [10] A. J. Van Dierendonck, "GPS Receivers," in *Global Positioning System: Theory and Applications*, W. P. Bradford and J. J. Spilker Jr., Eds. American Institute of Aeronautics and Astronautics, Inc., 1996.